Molecular Brain

RESEARCH Open Access

Shank3 deficiency alters midbrain GABAergic neuron morphology, GABAergic markers and synaptic activity in primary striatal neurons

Zuzana Bačová[1], Bohumila Jurkovičová-Tarabová[2,3], Tomáš Havránek[1,4], Denisa Mihalj[1], Veronika Borbélyová[5], Zdenko Pirnik[1,6], Boris Mravec[1,6], Daniela Ostatníková[6] and Ján Bakoš[1,6*]

Abstract

Abnormalities in gamma-aminobutyric acid (GABA)ergic neurotransmission play a role in the pathogenesis of autism, although the mechanisms responsible for alterations in specific brain regions remain unclear. Deficits in social motivation and interactions are core symptoms of autism, likely due to defects in dopaminergic neural pathways. Therefore, investigating the morphology and functional roles of GABAergic neurons within dopaminergic projection areas could elucidate the underlying etiology of autism. The aim of this study was to (1) compare the morphology and arborization of glutamate decarboxylase (GAD)-positive neurons from the midbrain tegmentum; (2) evaluate synaptic activity in primary neurons from the striatum; and (3) assess GABAergic postsynaptic puncta in the ventral striatum of wild-type (WT) and *Shank3*-deficient mice. We found a significant decrease in the number of short neurites in GAD positive primary neurons from the midbrain tegmentum in *Shank3*-deficient mice. The application of a specific blocker of $GABA_A$ receptors ($GABA_AR$) revealed significantly increased frequency of spontaneous postsynaptic currents (sPSCs) in *Shank3*-deficient striatal neurons compared to their WT counterparts. The mean absolute amplitude of the events was significantly higher in striatal neurons from *Shank3*-deficient compared to WT mice. We also observed a significant reduction in gephyrin/$GABA_AR$ *γ2* colocalization in the striatum of adult male *Shank3*-deficient mice. The gene expression of *collybistin* was significantly lower in the *nucleus accumbens* while *gephyrin* and *$GABA_AR$ γ2* were lower in the ventral tegmental area (VTA) in male *Shank3*-deficient compared to WT mice. In conclusion, *Shank3* deficiency leads to alterations in GABAergic neurons and impaired GABAergic function in dopaminergic brain areas. These changes may underlie autistic symptoms, and potential interventions modulating GABAergic activity in dopaminergic pathways may represent new treatment modality.

Keywords Autism spectrum disorder, Nucleus accumbens, Ventral tegmental area, GABA, *Shank3*, Neurite outgrowth

*Correspondence:
Ján Bakoš
j.bakos@savba.sk

Full list of author information is available at the end of the article

Introduction

Although alterations in gamma-aminobutyric acid (GABA)ergic inhibitory neurotransmission in autism are intensely studied [1, 2], it remains unclear how and in which brain regions changes in GABAergic neurons contribute to the development of autism. It is relatively well known how GABAergic interneurons proliferate, migrate, and reach their final destinations within the cortical and subcortical regions of the brain [3–5]. Nevertheless, GABAergic neurons are known to be present in the classical dopaminergic brain regions as well. For example, the ventral tegmental area (VTA) is composed of more than just dopamine producing cells, as approximately a third of the number of cells in the VTA are GABAergic neurons [6]. Besides local interneuron functions, GABAergic neurons from the VTA extend their projections to the striatum, particularly the *nucleus accumbens* (nAcc), as well as to other subcortical and cortical brain areas [7, 8]. These projections are part of the so-called long reward-associated neural circuits, which participate in the regulation of social interactions and social processing [2, 9]. Alterations in these neural circuits are likely linked to the pathogenesis of autism.

Investigating the morphology and functional roles of GABAergic neurons within dopaminergic projection areas could contribute to understanding the underlying etiology of autism. For this purpose, it is possible to use the well characterized model of SH3 and multiple ankyrin repeat domains 3 *(Shank3)*-deficient mice, which show autistic symptomatology [10, 11]. In our previous studies, we demonstrated that this autism-like model exhibits changes in neuritogenesis in neurons isolated from specific brain regions [12]. We also observed alterations in the markers of GABAergic neurons within dopaminergic areas of the brain [13]. However, it remains unclear how, or if, the morphology of GABAergic neurons in the dopaminergic brain regions is altered in *Shank3* deficient mice. Additionally, it is unknown whether there are any other changes in GABAergic inhibitory neurotransmission within the striatum in autism-like conditions.

Therefore, the aims of this study were to: (1) compare the morphology and arborization of primary glutamate decarboxylase (GAD)-positive primary neurons isolated from the midbrain tegmentum; (2) evaluate synaptic activity in primary neurons isolated from the striatum; and (3) assess GABAergic postsynaptic puncta in the ventral striatum (corresponding to the nAcc) of wild-type (WT) and *Shank3*-deficient mice. Additionally, gene expression of GABA receptor type A gamma subunit ($GABA_AR\ \gamma2$), *gephyrin* and *collybistin*, postsynaptic proteins important for clustering and anchoring of $GABA_AR$ at inhibitory synapses in the VTA and nAcc were evaluated in adult *Shank3*-deficient mice.

Materials and methods

Animals

In our experiments we used WT (C57BL/6J) and homozygous knockout ($Shank3^{-/-}$ here also called *Shank3*-deficient) mice generated by mating of *Shank3B* heterozygous mice (B6.129-$Shank3^{tm2Gfng/J}$) with PDZ depletion (exons 13 to 16) [10], obtained from the Jackson Laboratory (Stock No: 017688). Animals were kept on standard water supply and pelleted diet *ad libitum*. All experimental procedures were approved by the Ethical Committee of the Institute of Pathophysiology (07/2017/SKU11016), Comenius University, Bratislava, and have been conducted according to the European Union (EU) Directive 2010/63/EU and Slovak legislation.

Preparation of primary neurons

Primary neuronal cells from the striatal and tegmental area of WT and $Shank3^{-/-}$ mice (2–4 per group) were isolated on the first postnatal day (P0) according to the protocol by Reichova et al. [12]. Cells were planted into 24-well plates with individual 12 mm round poly-D-lysin pre-coated cover slips (10 µg/ml; Sigma-Aldrich, Germany) and incubated under standard condition (37 °C and 5% CO_2) in neuron-selective-growth medium (Neurobasal A; enriched with 2% B27 supplement (Invitrogen, USA); 100 U/ml penicillin; 100 U/ml streptomycin; 2 mM L-glutamine (all Gibco, USA)) for 5 days. Subsequently, 50% of the medium volume was replaced every two days.

Morphological analysis

Evaluation of morphological changes was performed on different days in vitro (DIV). On a given day, cells were fixed with 4% paraformaldehyde, pH 7.4 for 20 min at room temperature (RT). Coverslips were gently washed 3 times with ice-cold PBS and blocked for 30 min at RT in normal goat serum (3% NGS in PBS) with presence of 0.1% Triton X-100. Microtubule associated protein 2 (MAP2) and glutamate decarboxylase (GAD) 65/67 were detected with primary antibodies for 120 min at RT (concentration and source are presented in Table 1). After washing with ice-cold PBS (3 times) cells were incubated with corresponding fluorescent secondary antibody diluted in PBS (Table 2) for 60 min at RT. Cell nuclei were stained with 300 nM DAPI (4′,6-diamidino-2-phenylindole; Thermo Fisher Scientific, Germany) for 2 min.

Fluorescent images from two coverslips per animal were captured using an Olympus BX63 microscope at 20x magnification, maintaining consistent detection limits and utilizing automatic deconvolution. FIJI/IMAGE J software was used to evaluate at least 10 areas per coverslip. Cells that were immunopositively stained for both MAP2 and GAD65/67 were identified as GABAergic neurons. Dendritic arborization was analyzed using the Neuroanatomy/Sholl analysis plugin, which measured

Table 1 Primary antibodies

Name	Host species	Dilution	Method	Product number
anti-$GABA_AR$ γ2	Chicken	1:500	IHC	224,006, Synaptic System, Germany
anti-GAD65/67	Rabbit	1:500	ICC	ab11070; Abcam, UK
anti-GEPHYRIN	Rabbit	1:500	IHC	pa5-29036, Thermo Fisher Scientific, Germany
anti-MAP2	Mouse	1:2000	ICC	M4403; Sigma-Aldrich, Germany

Table 2 Fluorescent secondary antibodies

Name	Host species	Dilution	RRID
anti-mouse Alexa Fluor 488	Goat	1:500	A-11,001; Thermo Fisher Scientific, Germany
anti-rabbit Alexa Fluor 555	Goat	1:500	A-21,428; Thermo Fisher Scientific, Germany
anti-chicken Alexa Fluor 647	Goat	1:500	A-21,449; Thermo Fisher Scientific, Germany

the number of dendrite intersections with concentric circles at 1 µm intervals from the soma center up to 150 µm.

Spontaneous postsynaptic currents (sPSCs) in striatal neurons

Recordings were performed in a whole-cell configuration of the voltage-clamp at -70 mV using a HEKA EPC10 amplifier (HEKA Electronics). Acquisition and analysis were performed using Patchmaster v90.2. The input resistance and capacity transients were compensated by up to 70% with in-built circuits of the EPC 10 amplifier. Data were acquired at 10 kHz and filtered at 2,4 kHz. sPSCs were recorded in primary culture of striatal neurons on DIV 9–12. The extracellular solution used in the experiments contained (in millimolar): NaCl 127; KCl 2.5, $CaCl_2$ 2; $MgCl_2$ 1; HEPES 10; glucose 12; pH 7.4 (adjusted with NaOH). Patch pipettes had a resistance ranging from 2.8 MΩ to 3.5 MΩ when filled with a solution containing (in millimolar): CsCl 115; Mg-ATP 3; Na-GTP 0.5; TEACl 10; HEPES 25; EGTA 0.5; pH 7.2 (adjusted with CsOH). The osmolarity of the intracellular solution was approximately 300 mOsmol/L. During the recording, the specific antagonist of $GABA_A$ receptors, bicuculline (BIC) in 10 µM concentration was applied using a gravity flow perfusion system. Specific glutamate receptor blockers, 6-cyano-7- nitroquinoxaline-2,3-dione (CNQX, 10 µM) and D-2-amino-5-phosphonopentanoic acid (D-AP5, 20 µM) were applied to assess the character of the remaining sPSCs. Recorded sPSCs were analyzed offline using automatic detecting software Easy Electrophysiology and subsequently manually checked for accuracy. The detection threshold amplitude was set at 10 pA.

Quantitative real-time PCR

Brain tissues isolated from adult male mice ($n=6$/genotype) were used to analyze the expression of postsynaptic proteins and $GABA_AR$ γ2. Animals were sacrificed by decapitation and the brains were quickly removed from the skull; isolated tissues of nAcc and VTA were frozen on dry ice and stored at -70 °C. Total RNA was isolated by a phenol–chloroform method using TRI-reagent (MRC, Germany) according to the manufacturer's protocol. The reverse transcription procedure was carried out using the High-Capacity cDNA Reverse Transcription Kit (Thermo Fisher Scientific, Germany). qRT-PCR was processed using Power SYBR® Green PCR Master Mix (Thermo Fisher Scientific, Germany) on QuantStudio 5 thermocycler (Thermo Fisher Scientific, Germany). The $2^{-\Delta\Delta Ct}$ value of each sample was calculated using *Gapdh* or *S18* as reference control genes (sequences of primers in Table 3).

Table 3 List of primer sequences used in this study. $GABA_AR$ γ2 – gama 2 subunit of the $GABA_A$receptor, S18 – small ribosomal subunit, gapdh – glyceraldehyde 3-phosphate dehydrogenase

Name	Primers	Gene Bank	References
Collybistin	Fw: CAAGGAAACGGAAGAAGTGC	NM_001290385.1	[14]
	Rv: GGGCAGAGTTGACACCTTTC		
$GABA_AR$ γ2	Fw: ACTTCTGGTGACTATGTGGTGAT	NM_008073.4	[15]
	Rv: GGCAGGAACAGCATCCTTATTG		
Gapdh	Fw: CGGTGCTGAGTATGTCGTGGAGTC	NM_001289726.1	[16]
	Rv: CTTTTGGCTCCACCCTTCAAGTG		
Gephyrin	Fw: GACAGAGCAGTACGTGGAACTTCA	NM_145965.2	[17]
	Rv: GTCACCATCATAGCCGTCCAA		
S18	Fw: CGCCGCTAGAGGTGAAATTC	NR_003278.3	[18]
	Rv: TTGGCAAATGCTTTCGCTC		

Immunohistochemistry

For the determination of postsynaptic sites in the striatum of adult male WT and *Shank3*$^{-/-}$ mice (n=6 animals/group), we investigated the presence of GEPHYRIN and $GABA_AR$ γ2 colocalization. After the perfusion with 4% paraformaldehyde, pH 7.4, brains were stored overnight in the same fixative and then sectioned on the cryostat (CM1950, Leica Microsystems GmbH, Germany) at a thickness of 30 µm. Sections were temporarily stored (4 °C) in 24 well plates in PBS with 0.01% sodium azide. For immunohistochemistry, free-floating sections were blocked with 3% goat serum (NGS) and 0.01% Triton X-100 in PBS. After 1 h (RT), sections were incubated with a combination of primary antibodies: anti-GEPHYRIN and anti- $GABA_AR$ γ2 (Table 1) in PBS at 4 °C overnight. After washing with cold PBS (5 min/ 3times), sections were incubated with corresponding secondary antibodies (Table 2) diluted in PBS for 1.5 h at room temperature. Subsequent sections were rinsed with PBS (5 min / 3times), and 300 nM DAPI was added to stain the nuclei. After final PBS washing, sections were mounted on glass slides with Fluoromount-G (Sigma-Aldrich, Germany). GEPHYRIN- and $GABA_AR$ γ2 -stained sections were imaged by a Nikon confocal microscope (Nikon ECLIPSE Ti-E, A1R+; Netherlands). Free-floating sections (30 µm thick) were imaged at high magnification (40x objective, numerical aperture 1.3; resolution 1024×1024 pixels) at 0.5 µm steps. Quantification of colocalization between GEPHYRIN and $GABA_AR$ γ2 was performed using the Fiji/ImageJ plugin ComDet v0.4.1 [19]. In brief, particles were detected from three different areas of the nAcc in both 555 and 647 channels independently with an approximate size of 3 pixels and an intensity threshold of 3 SD. Colocalization was determined based on the maximum distance of 1 pixel between particles.

Statistical analysis

Statistical analyses were performed using GraphPad Prism 10.2.3. The data for gene expressions, morphology analysis and colocalizations were first tested for normal distribution using the Shapiro–Wilk test. Comparisons of relative gene expression were performed using the Mann-Whitney non- parametric test. Two-way ANOVA (genotype, arborization) was used for morphological changes analysis, with Sidac test as a *post hoc*. For a colocalization evaluation, data points that fell below Q1−1.5 * IQR or above Q3+1.5 * IQR were considered outliers and were therefore excluded from the analysis. Changes in colocalization of GEPHYRIN and $GABA_AR$ γ2 postsynaptic puncta were evaluated by Student T test. For electrophysiology measurements, outliers were identified using ROUT method. Cleared data were subsequently tested for normality using D`Agostino & Pearson test and a comparison of data for two groups was performed by Mann-Whitney non-parametric test. Results are expressed as the mean±SEM. The value of $p<0.05$ was considered statistically significant.

Results

Primary neuronal cultures isolated from midbrains of WT and *Shank3*-deficient mice were used to evaluate morphological changes in GAD-positive neurons on days 3, 5, and 7 in vitro. Neurite number and branching were assessed using Sholl analysis. Two-way ANOVA was performed for the independent factors (1) genotype and (2) distance from the cell nucleus, separately at each time point. On the DIV3, two-way ANOVA showed no significant effects of factor genotype, but neurite arborization was clearly different ($F_{(150,\ 14797)}=112.5$; $p<0.001$) depending on the distance from the nucleus (Fig. 1). On DIV5, statistical analysis revealed significant interaction between tested factors ($F_{(150,\ 11778)}=2.072$; $p<0.001$). Significant effects of factors genotype ($F_{(1,\ 11778)}=12.88$; $p<0.001$) and distance ($F_{(150,\ 11778)}=39.87$; $p<0.001$) were observed. Based on Sidac post hoc test, neurons isolated from *Shank3*-deficient mice exhibited a significantly lower number of shorter neurites within specific distance ranges (19–30 µm). Simultaneously, it was observed that at larger distances from the nucleus, neurite arborization was increased in neurons isolated from *Shank3*-deficient compared to WT mice. A similar significant trend was also observed on DIV7 where there were significant effects of the genotype ($F_{(1,\ 11778)}=206.6$; $p<0.001$), distance from the nucleus ($F_{(150,\ 11778)}=100.7$; $p<0.001$), as well as the interaction of these factors ($F_{(150,\ 11778)}=1.35$; $p<0.001$).

To determine whether changes in neurite outgrowth from midbrain GABAergic neurons have functional consequences for spontaneous postsynaptic activity in the projection area, we employed the isolated primary neurons from the striatum of WT and *Shank3*-deficient mice. sPSCs recorded at -70 mV in control conditions showed marked although non-significant increased frequency in neurons from *Shank3*-deficient mice compared to WT mice neurons (Fig. 2A). BIC treatment revealed a portion of spontaneous postsynaptic currents indicating GABAergic activity (Fig. 2D). sPSCs with BIC application were notably increased in *Shank3*-deficient striatal neurons compared to WT counterparts (Fig. 2A, B). The mean absolute amplitude of the events was significantly higher in striatal neurons from *Shank3*-deficient mice compared to WT when recorded under control conditions (Fig. 2C). The application of BIC had no significant effect on the mean event amplitude neither in WT neurons nor in *Shank3*-deficient mice neurons.

In relation to inhibitory neurotransmission, we conducted an analysis of the colocalization of GABA

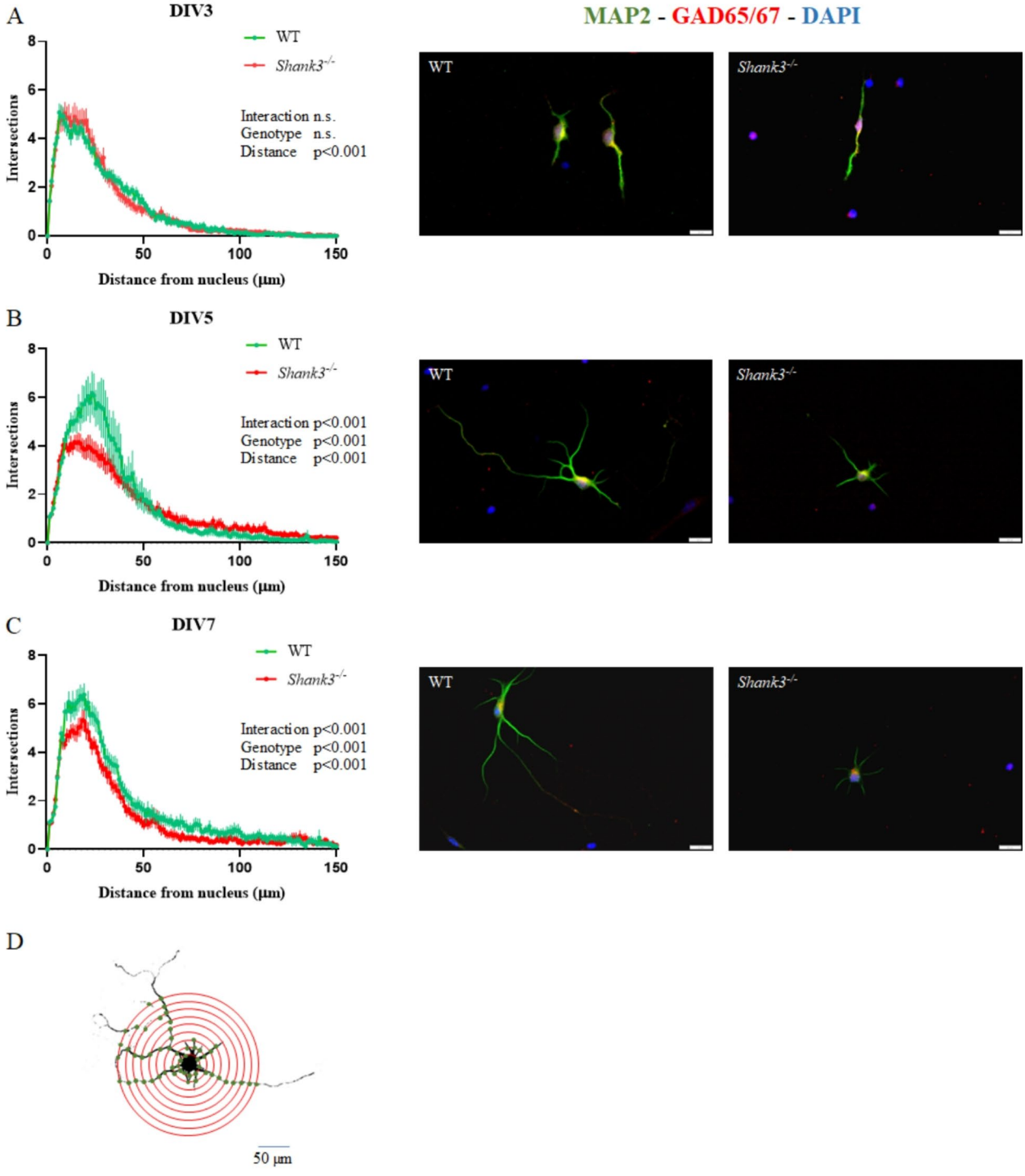

Fig. 1 Dendritic arborization in primary glutamate decarboxylase (GAD) positive tegmental neurons isolated from WT and *Shank3*-deficient mice. Neurons were maintained in neuron-selective-growth medium and stained on 3rd, 5th and 7th day in vitro (DIV3, DIV5 and DIV7). Microtubule associated protein 2 (MAP2) served as a marker for neurons, whereas GAD65/67 was utilized to specifically identify GABAergic neurons. Cell nuclei were stained with DAPI. The arborization of the dendritic tree was assessed using Sholl analysis. The number of dendrite intersections (mean ± SEM) for various concentric circles are represented on graphs on DIV3 (**A**, $n = 50$ neurons/genotype), DIV5 (**B**, $n = 40$/ neurons/genotype) and DIV7 (**C**, $n = 40$ neurons/genotype) with representative images of neurons labelled for MAP2 (green), GAD65/67 (red), and DAPI (blue). Representative image (**D**) shows a neuron in binary black and white display with concentric circles. Statistical differences between groups were determined by two-way ANOVA for factors (1) genotype and (2) distance from the cell nucleus. WT - wild type

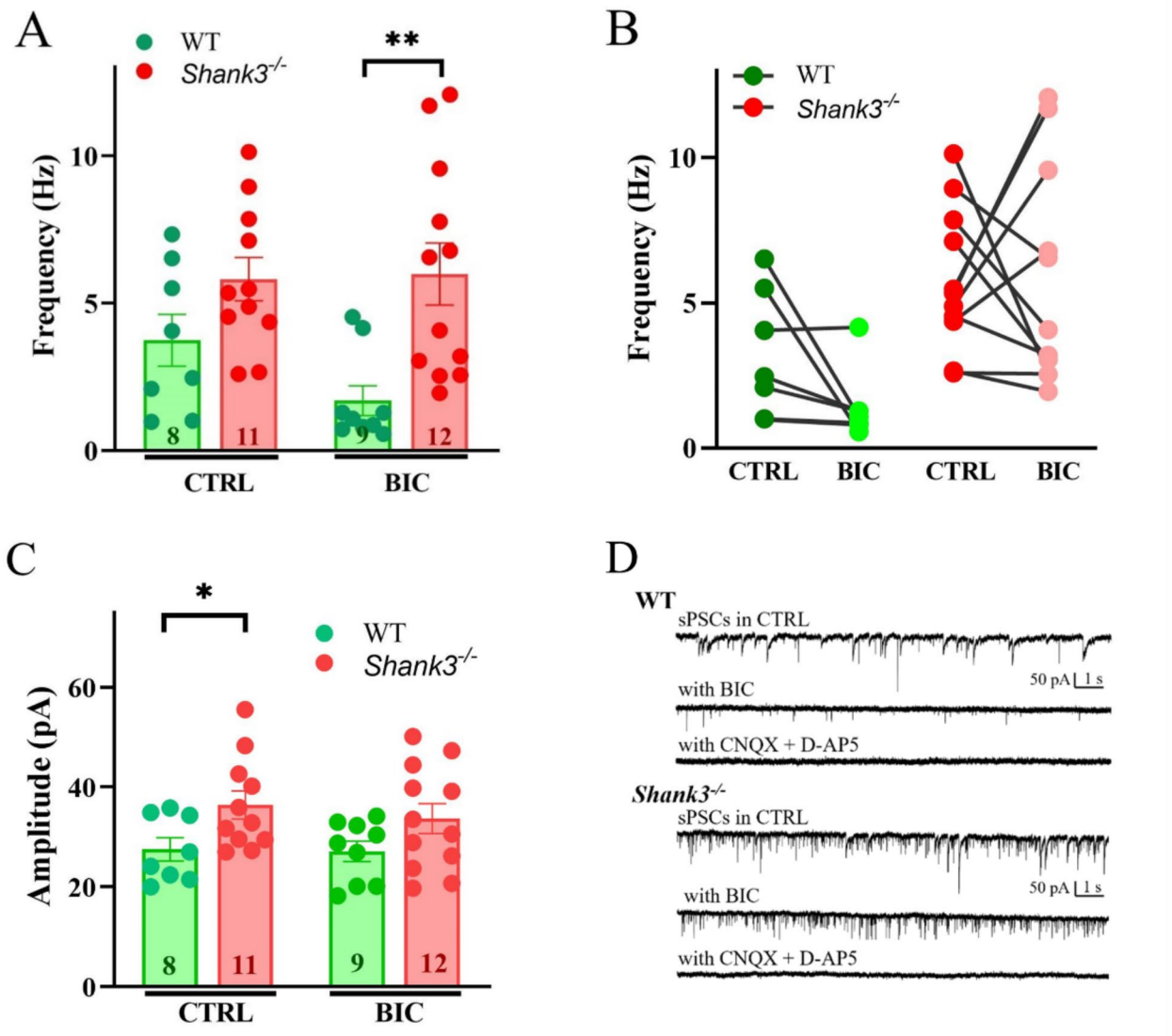

Fig. 2 Spontaneous postsynaptic currents (sPSCs) in striatal neurons from wild-type and *Shank3*-deficient mice. (**A**) Averaged frequencies of sPSCs recorded at -70 mV in control extracellular solution (CTRL) and under bicuculline (BIC) treatment in WT and *Shank3*-deficient mice neurons. Data are presented as mean ± SEM (**$p < 0.01$). (**B**) Change of sPSCs frequency values for individual WT ($n = 7$) and *Shank3*-deficient ($n = 11$) neurons in control conditions and with the application of BIC. (**C**) Averaged absolute amplitude of sPSC events from WT and *Shank3*-deficient neurons in control conditions and with the application of BIC (*$p < 0.05$). (**D**) Representative sPSC traces recorded from WT and *Shank3*-deficient neurons in control extracellular solution, with the application of BIC and following application of the specific glutamate receptor blockers CNQX (10 μM) and D-AP5 (20 μM)

postsynaptic markers in the nAcc of adult WT and *Shank3*-deficient mice. A significant reduction (Student T test, p˂0.01, T = 3.104, df = 521) in the colocalization of GEPHYRIN/$GABA_AR$ γ2 postsynaptic puncta in the striatum of *Shank3*-deficient compared to WT mice was revealed (Fig. 3A). To assess whether alterations in GABAergic postsynaptic puncta in the nAcc of *Shank3*-deficient mice are associated with specific $GABA_AR$ related postsynaptic proteins, we analyzed *gephyrin*, *collybistin* and *$GABA_AR$ γ2* gene expression in the VTA and nAcc. The gene expression of *collybistin* was significantly (Mann-Whitney, p˂0.05, U = 1, df = 9) decreased in the nAcc and *gephyrin* in the VTA (Mann-Whitney, p˂0.05, U = 5, df = 10) in *Shank3* deficient compared to WT mice (Fig. 4). Gene expression of *$GABA_AR$ γ2* was significantly decreased (Mann-Whitney, p˂0.01, U = 1, df = 8) in the VTA of *Shank3*-deficient compared to WT mice.

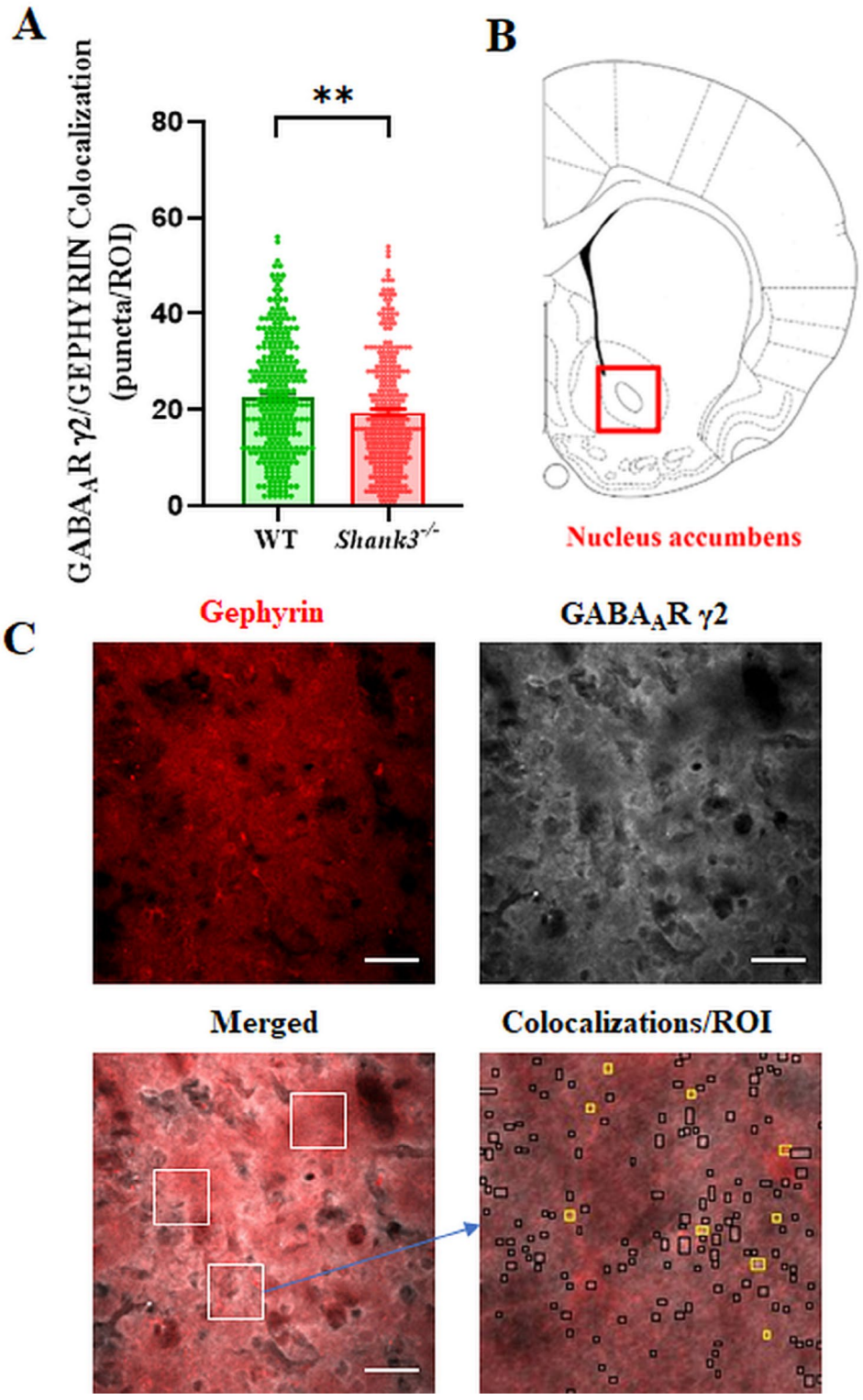

Fig. 3 Effect of *Shank3* deficiency on the colocalization of GEPHYRIN/ GABA$_A$R γ2 postsynaptic puncta in the *nucleus accumbens*. **A**) Statistical significance between medians of colocalized particles (ROI = 294/genotype) was determined using the Student T test (**$p < 0.01$). Number of mice: $N = 6$/genotype. Data are presented as mean ± SEM (**B**) Schematic representation of the chosen region (*nucleus accumbens*) and (**C**) confocal microscopy image (40x magnification) showing immunoreactivity to GEPHYRIN (red) and GABA$_A$R γ2 (white), as well as image of their colocalization (yellow sqaures) in coronal brain slices. Scale bars represent 50 µm; white box (60 × 60 µm)

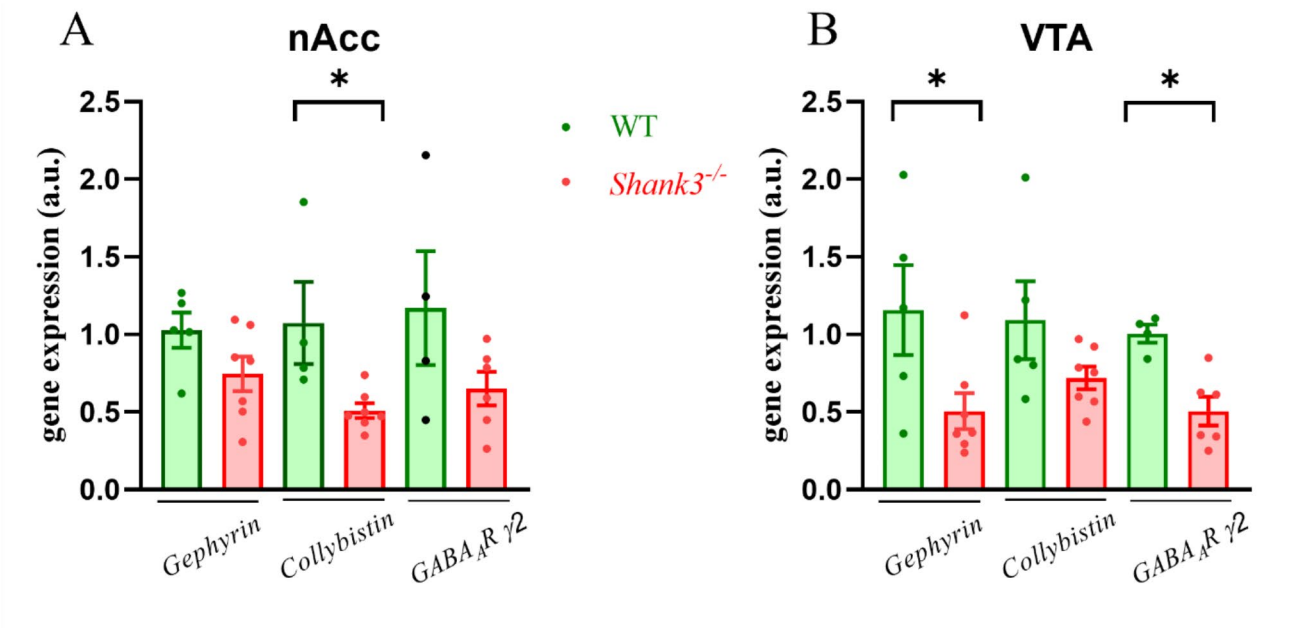

Fig. 4 Changes in the gene expression levels of postsynaptic proteins and GABA receptor subunit in the *nucleus accumbens* (nAcc) and ventral tegmental area (VTA) isolated from WT and *Shank3*-deficient male mice. Graphs show relative mRNA expressions. Figures represent relative changes compared to the WT group calculated by $2^{-\Delta\Delta Ct}$ method. *Glyceraldehyde 3-phosphate dehydrogenase* or *S18* were selected as the reference genes. Column scatter dot plot represents values of individual samples and bar represents means ± SEM ($n = 4–6$). Significantly different values are marked with $*p < 0.05$, Mann-Whitney, WT - wild type. $GABA_AR$ γ2 – gamma 2 subunit of the $GABA_A$ receptor, S18 – small ribosomal subunit

Discussion

In the present study, we observed significant changes in the neurite outgrowth and branching of GAD-positive primary neurons isolated from the tegmental area of the midbrain in *Shank3*-deficient mice. We also detected a notable reduction of GABAergic postsynaptic puncta and selected postsynaptic proteins in the dopaminergic brain regions of *Shank3*-deficient mice, which was accompanied by enhanced spontaneous postsynaptic activity in isolated striatal neurons.

The finding that *Shank3*-deficient mice exhibit altered arborization of GABAergic neurons isolated from the midbrain suggests changes in neurite growth and synaptic connections, potentially affecting signal processing in dopaminergic brain regions under autism-like conditions. It is well known that abnormal connectivity in dopaminergic pathways contributes to the pathogenesis of autism [3, 20]. Moreover, recent studies point to long-range connections of GABAergic neurons that intertwine with VTA dopaminergic neurons [21, 22]. It is therefore possible that insufficient growth of midbrain GABAergic neurons results in functional striatal abnormalities in *Shank3*-deficient mice. In our study, we surprisingly found a significantly higher amplitude of sPSCs in striatal neurons from *Shank3*-deficient mice when recorded under control conditions. The application of BIC had no significant effect on the amplitude neither in WT neurons nor in *Shank3*-deficient mice neurons. Since SHANK3 is localized in postsynaptic endings, it is possible that these signals are the result of tonic disinhibition of striatal neurons in vitro as these neurons are regulated by dopamine release under in vivo conditions [23]. It is important to note that GABAergic neurons from the VTA are believed to project to nAcc interneurons [24]. A limitation of our approach is that we did not distinguish the phenotype of the evaluated neurons, despite the known presence of medium spiny neurons. Moreover, the consequences of *Shank3*-deficiency-related synaptopathy in striatal neurons can be cell-specific [25]. Most studies indicate reduced inhibitory currents or altered excitatory/inhibitory balance in the striatum in autistic model tissues [10, 26, 27]. However, it is important to note, that GABAergic conductance in the striatum exhibits considerable heterogeneity and variation and may be even more pronounced under pathological conditions [28].

In this study, the observed increase in the frequency of sPSCs under BIC in striatal neurons isolated from *Shank3*-deficient mice may suggest that there are more excitatory postsynaptic currents occurring spontaneously. Although, in our study, these are isolated primary striatal neurons and not the entire tissue, which means we cannot determine the precise presynaptic cause of these observations, it is possible that the reduction of inhibitory input allows for more frequent firing of excitatory neurons. sPSCs in striatal cells from *Shank3*-deficient mice may be related to the observed decrease in

GEPHYRIN/$GABA_AR$ γ2 colocalization in the nAcc. Gephyrin is a key scaffolding protein essential for stabilizing GABA receptors at inhibitory synapses [29]. Reduced colocalization of GEPHYRIN/$GABA_AR$ could lead to a compensatory increase in excitatory synaptic activity [30]. This suggests that the structural changes at the synapse due to reduced GEPHYRIN and $GABA_AR$ interaction may drive functional alterations in synaptic transmission. Another indicator of GABAergic synapse remodeling in the striatum is the decreased expression of *collybistin* in the nAcc observed in this study. Collybistin interacts with gephyrin and is involved in the clustering of $GABA_ARs$ [31]. In autistic conditions, the disassembly of these complexes has been suggested [32, 33]. Notably, bilateral GABAergic projections from the VTA to the striatum, as well as from the striatum to the VTA, are implicated in pathogenesis of autism. Thus, the remodeling of GABAergic synapses in these areas may be induced by *Shank3* deficiency. Other studies have shown an abnormal striatal neuronal morphology in *Shank3*-deficient mice [10]. These neurons are involved in microcircuits within the striatum and also participate in long-range cortical projections to and from the midbrain [34]. Although Peca et al. [10] noted an increase in the complexity of dendritic arborization in *Shank3*-deficient mice using Sholl analysis, our findings indicate, on the contrary, a decrease in the number of short neurites, especially in GAD positive neurons in the midbrain tegmentum. Other studies have also found that SHANK3 knockdown in human induced pluripotent stem cells can lead to a decrease in dendritic arborization [35]. Moreover, shortened neurite outgrowth in primary hippocampal neurons isolated from *Shank3*-deficient mice was previously demonstrated [12].

In conclusion, *Shank3* deficiency seems to cause alterations in GABAergic neurons, leading to impaired GABAergic function, as observed in two other *Shank3*-deficient models [36]. Our electrophysiological data also confirm that the inhibition of $GABA_ARs$ leads to increased synaptic activity of striatal neurons from *Shank3*-deficient mice, highlighting the well-known excitation/inhibition imbalance in the context of autism. This interpretation is further supported by the reduction of GABAergic postsynaptic puncta in the striatum of *Shank3*-deficient mice in this study, which corresponds to previous findings observed in the piriform cortex [14]. Similarly, human postmortem ASD samples revealed reduced numbers of cortical GABAergic interneurons and altered branching, correlating with core autism symptoms such as repetitive behaviors and motor stereotypies [37]. Morphological and functional properties of GABAergic neurons that originate from the midbrain and project to the striatum require further investigation, particularly in the context of behavioral changes associated with autism.

Acknowledgements
We thank Dr. Zuzana Ševčíková Tomášková for her valuable advice on the statistical analysis of electrophysiological data.

Author contributions
All authors had full access to all the data in the study and take responsibility for the integrity of the data and the accuracy of the data analysis. Conceptualization: J.B.; Investigation: Z.B.; V.B.; Z.P.; B.M., B.T.; D.M.; T.H.; Z.B.; J.B.; Resources: Z.B.; B.T., T.H.; J.B.; Writing - Original Draft: Z.B.; B.T.; J.B. Writing - Review & Editing: D.O. ; Z.B.; J.B.; Funding Acquisition: J.B.

Funding
This work was supported by projects 2/0057/23 of the Grant Agency of the Ministry of Education and Slovak Academy of Sciences (VEGA) and by the Slovak Research and Development Agency projects APVV-21-0189.

Data availability
The data that support the findings of this study are available from the corresponding author upon reasonable request.

Declarations

Ethics approval and consent to participate
All experimental procedures were approved by the Ethical Committee of the Institute of Pathophysiology (07/2017/SKU11016), Comenius University, Bratislava, and have been conducted according to the European Union (EU) Directive 2010/63/EU and Slovak legislation.

Consent for publication
Not applicable.

Competing interests
Authors declare no conflict of interest.

Author details
[1]Institute of Experimental Endocrinology, Biomedical Research Center, Slovak Academy of Sciences, Dubravska cesta 9, Bratislava 845 05, Slovakia
[2]Institute of Molecular Physiology and Genetics, Center of Biosciences, Slovak Academy of Sciences, Bratislava, Slovakia
[3]Department of Biology, Faculty of Education, Trnava University, Trnava, Slovakia
[4]Institute of Anatomy, Faculty of Medicine, Comenius University in Bratislava, Bratislava, Slovakia
[5]Institute of Molecular Biomedicine, Faculty of Medicine, Comenius University in Bratislava, Bratislava, Slovakia
[6]Institute of Physiology, Faculty of Medicine, Comenius University in Bratislava, Sasinkova 2, Bratislava 813 72, Slovakia

Received: 18 July 2024 / Accepted: 12 September 2024
Published online: 27 September 2024

References

1. Puts NAJ, Wodka EL, Harris AD, Crocetti D, Tommerdahl M, Mostofsky SH, Edden RAE. Reduced GABA and altered somatosensory function in children with autism spectrum disorder. Autism Res. 2017;10(4):608–19. https://doi.org/10.1002/aur.1691. Epub 2016 Sep 9.
2. Parrella NF, Hill AT, Dipnall LM, Loke YJ, Enticott PG, Ford TC. Inhibitory dysfunction and social processing difficulties in autism: a comprehensive narrative review. J Psychiatr Res. 2024;169:113–25. Epub 2023 Nov 18.
3. Havranek T, Bacova Z, Bakos J. Oxytocin, GABA, and dopamine interplay in autism. Endocr Regul. 2024;58(1):105–14. https://doi.org/10.2478/enr-2024-0012

4. Zhu Y, Li H, Zhou L, Wu JY, Rao Y. Cellular and molecular guidance of GABAergic neuronal migration from an extracortical origin to the neocortex. Neuron. 1999;23(3):473–85. https://doi.org/10.1016/s0896-6273(00)80801-6
5. Tang X, Jaenisch R, Sur M. The role of GABAergic signalling in neurodevelopmental disorders. Nat Rev Neurosci. 2021;22(5):290–307. https://doi.org/10.1038/s41583-021-00443-x. Epub 2021 Mar 26.
6. Bouarab C, Thompson B, Polter AM. VTA GABA neurons at the interface of stress and reward. Front Neural Circuits. 2019;13:78. https://doi.org/10.3389/fncir.2019.00078
7. Root DH, Barker DJ, Estrin DJ, Miranda-Barrientos JA, Liu B, Zhang S, Wang HL, Vautier F, Ramakrishnan C, Kim YS, Fenno L, Deisseroth K, Morales M. Distinct signaling by ventral tegmental area glutamate, GABA, and combinatorial Glutamate-GABA neurons in motivated behavior. Cell Rep. 2020;32(9):108094. https://doi.org/10.1016/j.celrep.2020.108094
8. Chuhma N, Oh SJ, Rayport S. The dopamine neuron synaptic map in the striatum. Cell Rep. 2023;42(3):112204. https://doi.org/10.1016/j.celrep.2023.112204. Epub 2023 Mar 2. PMID: 36867530; PMCID: PMC10657204.
9. Faget L, Oriol L, Lee WC, Zell V, Sargent C, Flores A, Hollon NG, Ramanathan D, Hnasko TS. Ventral pallidum GABA and glutamate neurons drive approach and avoidance through distinct modulation of VTA cell types. Nat Commun. 2024;15(1):4233. https://doi.org/10.1038/s41467-024-48340-y
10. Peça J, Feliciano C, Ting JT, Wang W, Wells MF, Venkatraman TN, Lascola CD, Fu Z, Feng G. Shank3 mutant mice display autistic-like behaviours and striatal dysfunction. Nature. 2011;472(7344):437–42. https://doi.org/10.1038/nature09965. Epub 2011 Mar 20.
11. Bey AL, Wang X, Yan H, Kim N, Passman RL, Yang Y, Cao X, Towers AJ, Hulbert SW, Duffney LJ, Gaidis E, Rodriguiz RM, Wetsel WC, Yin HH, Jiang YH. Brain region-specific disruption of Shank3 in mice reveals a dissociation for cortical and striatal circuits in autism-related behaviors. Transl Psychiatry. 2018;8(1):94. https://doi.org/10.1038/s41398-018-0142-6
12. Reichova A, Bacova Z, Bukatova S, Kokavcova M, Meliskova V, Frimmel K, Ostatnikova D, Bakos J. Abnormal neuronal morphology and altered synaptic proteins are restored by oxytocin in autism-related SHANK3 deficient model. Mol Cell Endocrinol. 2020;518:110924. https://doi.org/10.1016/j.mce.2020.110924. Epub 2020 Jun 30.
13. Bukatova S, Renczes E, Reichova A, Filo J, Sadlonova A, Mravec B, Ostatnikova D, Bakos J, Bacova Z. Shank3 deficiency is associated with altered profile of neurotransmission markers in pups and adult mice. Neurochem Res. 2021;46(12):3342–55. https://doi.org/10.1007/s11064-021-03435-6. Epub 2021 Aug 28.
14. Mihalj D, Borbelyova V, Pirnik Z, Bacova Z, Ostatnikova D, Bakos J. Shank3 deficiency results in a reduction in GABAergic postsynaptic puncta in the olfactory brain areas. Neurochem Res. 2024;49(4):1008–16. https://doi.org/10.1007/s11064-023-04097-2. Epub 2024 Jan 6.
15. Bhandage AK, Friedrich LM, Kanatani S, Jakobsson-Björkén S, Escrig-Larena JI, Wagner AK, Chambers BJ, Barragan A. GABAergic signaling in human and murine NK cells upon challenge with toxoplasma gondii. J Leukoc Biol. 2021;110(4):617–28. https://doi.org/10.1002/JLB.3HI0720-431R. Epub 2021 May 24.
16. Arsenault J, Gholizadeh S, Niibori Y, Pacey LK, Halder SK, Koxhioni E, Konno A, Hirai H, Hampson DR. FMRP expression levels in mouse central nervous system neurons determine behavioral phenotype. Hum Gene Ther. 2016;27(12):982–96. https://doi.org/10.1089/hum.2016.090
17. Du Z, Tertrais M, Courtand G, Leste-Lasserre T, Cardoit L, Masmejean F, Halgand C, Cho YH, Garret M. Differential alteration in expression of striatal GABAAR subunits in mouse models of Huntington's disease. Front Mol Neurosci. 2017;10:198. https://doi.org/10.3389/fnmol.2017.00198
18. Yoon S, Choi YC, Lee S, Jeong Y, Yoon J, Baek K. Induction of growth arrest by mir-542-3p that targets survivin. FEBS Lett. 2010;584(18):4048–52. https://doi.org/10.1016/j.febslet.2010.08.025
19. Bottermann M, Foss S, Caddy SL, Clift D, van Tienen LM, Vaysburd M, Cruickshank J, O'Connell K, Clark J, Mayes K, Higginson K, Lode HE, McAdam MB, Sandlie I, Andersen JT, James LC. Complement C4 prevents viral infection through capsid inactivation. Cell Host Microbe. 2019;25(4):617–e6297. https://doi.org/10.1016/j.chom.2019.02.016
20. Sato M, Nakai N, Fujima S, Choe KY, Takumi T. Social circuits and their dysfunction in autism spectrum disorder. Mol Psychiatry. 2023;28(8):3194–206. https://doi.org/10.1038/s41380-023-02201-0. Epub 2023 Aug 24.
21. Cai J, Tong Q. Anatomy and function of ventral tegmental area glutamate neurons. Front Neural Circuits. 2022;16:867053. https://doi.org/10.3389/fncir.2022.867053
22. Chowdhury S, Matsubara T, Miyazaki T, Ono D, Fukatsu N, Abe M, Sakimura K, Sudo Y, Yamanaka A. GABA neurons in the ventral tegmental area regulate non-rapid eye movement sleep in mice. Elife. 2019;8:e44928. https://doi.org/10.7554/eLife.44928
23. Gantz SC, Bunzow JR, Williams JT. Spontaneous inhibitory synaptic currents mediated by a G protein-coupled receptor. Neuron. 2013;78(5):807–12. https://doi.org/10.1016/j.neuron.2013.04.013
24. Morales M, Margolis EB. Ventral tegmental area: cellular heterogeneity, connectivity and behaviour. Nat Rev Neurosci. 2017;18(2):73–85. https://doi.org/10.1038/nrn.2016.165
25. Wang YZ, Perez-Rosello T, Smukowski SN, Surmeier DJ, Savas JN. Neuron type-specific proteomics reveals distinct Shank3 proteoforms in iSPNs and dSPNs lead to striatal synaptopathy in Shank3B-/- mice. Mol Psychiatry. 2024 Mar 14. https://doi.org/10.1038/s41380-024-02493-w. Epub ahead of print. Erratum in: Mol Psychiatry. 2024 Mar 28. https://doi.org/10.1038/s41380-024-02543-3.
26. Li W, Pozzo-Miller L. Dysfunction of the corticostriatal pathway in autism spectrum disorders. J Neurosci Res. 2020;98(11):2130–47. https://doi.org/10.1002/jnr.24560. Epub 2019 Nov 22.
27. Jaramillo TC, Speed HE, Xuan Z, Reimers JM, Liu S, Powell CM. Altered striatal synaptic function and abnormal behaviour in Shank3 Exon4-9 deletion mouse model of autism. Autism Res. 2016;9(3):350–75. https://doi.org/10.1002/aur.1529. Epub 2015 Nov 11.
28. Lee V, Maguire J. The impact of tonic GABAA receptor-mediated inhibition on neuronal excitability varies across brain region and cell type. Front Neural Circuits. 2014;8:3. https://doi.org/10.3389/fncir.2014.00003. PMID: 24550784; PMCID: PMC3909947.
29. Sassoè-Pognetto M, Panzanelli P, Sieghart W, Fritschy JM. Colocalization of multiple GABA(A) receptor subtypes with gephyrin at postsynaptic sites. J Comp Neurol. 2000;420(4):481–98.
30. Tretter V, Mukherjee J, Maric HM, Schindelin H, Sieghart W, Moss SJ. Gephyrin, the enigmatic organizer at GABAergic synapses. Front Cell Neurosci. 2012;6:23. https://doi.org/10.3389/fncel.2012.00023
31. George S, Bear J Jr, Taylor MJ, Kanamalla K, Fekete CD, Chiou TT, Miralles CP, Papadopoulos T, De Blas AL. Collybistin SH3-protein isoforms are expressed in the rat brain promoting gephyrin and GABA-A receptor clustering at GABAergic synapses. J Neurochem. 2021;157(4):1032–51. https://doi.org/10.1111/jnc.15270
32. Machado CO, Griesi-Oliveira K, Rosenberg C, Kok F, Martins S, Passos-Bueno MR, Sertie AL. Collybistin binds and inhibits mTORC1 signaling: a potential novel mechanism contributing to intellectual disability and autism. Eur J Hum Genet. 2016;24(1):59–65. https://doi.org/10.1038/ejhg.2015.69
33. Chiou TT, Long P, Schumann-Gillett A, Kanamarlapudi V, Haas SA, Harvey K, O'Mara ML, De Blas AL, Kalscheuer VM, Harvey RJ. Mutation p.R356Q in the collybistin phosphoinositide binding site is associated with mild intellectual disability. Front Mol Neurosci. 2019;12:60. https://doi.org/10.3389/fnmol.2019.00060
34. Melzer S, Monyer H. Diversity and function of corticopetal and corticofugal GABAergic projection neurons. Nat Rev Neurosci. 2020;21(9):499–515. https://doi.org/10.1038/s41583-020-0344-9. Epub 2020 Aug 3.
35. Huang G, Chen S, Chen X, Zheng J, Xu Z, Doostparast Torshizi A, Gong S, Chen Q, Ma X, Yu J, Zhou L, Qiu S, Wang K, Shi L. Uncovering the functional link between SHANK3 deletions and deficiency in neurodevelopment using iPSC-derived human neurons. Front Neuroanat. 2019;13:23. https://doi.org/10.3389/fnana.2019.00023
36. Filice F, Vörckel KJ, Sungur AÖ, Wöhr M, Schwaller B. Reduction in parvalbumin expression not loss of the parvalbumin-expressing GABA interneuron subpopulation in genetic parvalbumin and shank mouse models of autism. Mol Brain. 2016;9:10. https://doi.org/10.1186/s13041-016-0192-8
37. Dufour BD, McBride E, Bartley T, Juarez P, Martínez-Cerdeño V. Distinct patterns of GABAergic interneuron pathology in autism are associated with intellectual impairment and stereotypic behaviors. Autism. 2023;27(6):1730–45. https://doi.org/10.1177/13623613231154053

Publisher's note